CVD GROWTH AND CHARACTERIZATION OF MULTILAYER GRAPHENE DOMAINS ON COPPER WITH POLYMER-ASSISTED TRANSFER ONTO SiO_2/Si SUBSTRATES

Oybek Tursunkulov[1], Gulmira Khojieva[2], Mirazim Sobitov[2], Bahodir Gulyamov[1], Soyibjon Bozorov[1], Shokir Khojiev[1], **Khamdam Akbarov[2]****

[1] **Center for Advanced Technology** under the Ministry of Higher Education, Science and Innovation of the Republic of Uzbekistan, Tashkent 100174, Uzbekistan [2] **Faculty of Chemistry, National University of Uzbekistan**, Tashkent 100174, Uzbekistan

ABSTRACT

This work presents the synthesis of multilayer graphene domains on copper substrates by thermal chemical vapor deposition (CVD). A detailed description of the CVD reactor system is provided, including the use of argon as a cooling medium and methane as the carbon precursor. Optimal process parameters temperature regimes, gas flow rates, working pressure, and cooling profiles were experimentally determined. Surface morphology was examined using optical and field-emission scanning electron microscopy, revealing discrete rectangular graphene domains with heterogeneous orientations. Raman spectroscopy confirmed the multilayer nature of the domains, the presence of structural defects, and variations in crystallinity. PMMA-assisted transfer of graphene onto SiO_2/Si substrates was also investigated; microscopy revealed the presence of polymer residues, wrinkles, and surface contamination. These findings demonstrate both the effectiveness of thermal CVD for producing domain-structured multilayer graphene and the limitations of polymer-mediated transfer. The results contribute to improving synthesis and transfer strategies for advanced graphene-based electronic, sensing, and energy devices.
Keywords: Multilayer graphene domains, CVD, copper foil, silicon substrate.

INTRODUCTION

Graphene, owing to its unique properties high electrical and thermal conductivity, optical transparency, and mechanical strength has attracted significant interest for a wide range of applications. Since the first experiments on the synthesis of multilayer graphene [1,2], numerous studies have been published addressing its properties and production technologies. This innovative material is now widely utilized across various fields of science and engineering [3–10]. In particular, it is employed in photovoltaics [11–13] as a component of solar cells due to its transparency and conductivity; in field-effect transistors [14,16] due to the high mobility of charge carriers; in flexible transparent electrodes [17–19]; in gas sensors [20–24] owing to its high sensitivity to gas molecules; as well as in magnetic and optical systems [25–28]. Moreover, graphene holds considerable promise for advances in catalysis and hydrogen energy technologies [29–35], where it can serve as a modified structure for efficient catalysts and hydrogen storage systems. Various techniques for graphene synthesis based on different equipment and technological approaches have been developed. The most well-known among them include mechanical exfoliation of graphite [36,37]; epitaxial synthesis based on thermal graphitization of monocrystalline silicon carbide surfaces [38,39]; and chemical routes involving the synthesis of graphene oxide dispersed in solution, followed by hydrazine reduction [40,41]. The chemical vapor deposition (CVD) method on metal surfaces is considered the most promising approach for the industrial-scale fabrication of large-area graphene samples due to its cost-effectiveness, efficiency, and high material quality [41–47]. The aim of the present study is to develop a technology for obtaining discrete graphene domains on a copper substrate using chemical vapor deposition, followed by analysis of the surface morphology and structural characteristics of the synthesized samples.

METHODOLOGY

Chemical vapor deposition (CVD) is one of the key technologies for producing high-quality thin films, including graphene a single- or few-layer carbon material possessing exceptional electrical and mechanical properties. Thermal Chemical Vapor Deposition (thermal CVD) stands out among other methods due to its reliance on substrate heating to initiate chemical reactions, making it particularly suitable for graphene synthesis, especially on copper substrates. This type of equipment is also widely used in the semiconductor industry, in the fabrication of optical components, solar cells, nanostructures (such as graphene and carbon nanotubes), and protective coatings. Figure 1 shows a thermal CVD system, which consists of seven components. The central element of the system is a horizontal thermal reactor (1), comprising a heating furnace where the deposition process takes place. Positioned beneath the reactor is a programmable control unit (2), which enables full automation of the process by regulating heating and cooling temperatures, pressure, and gas flow rates to optimize the synthesis conditions (see in figure 1).

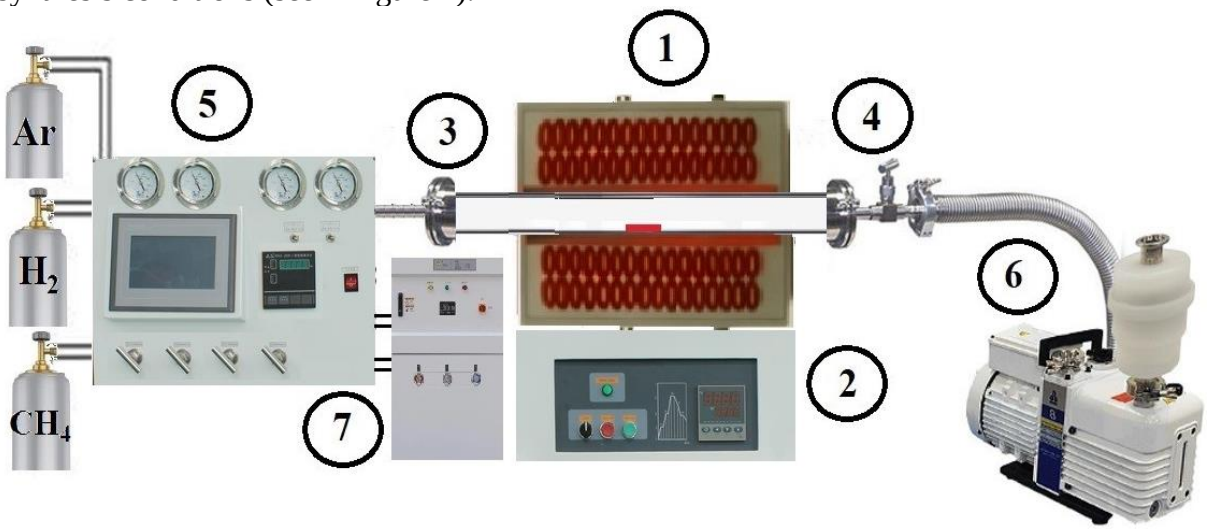

Figure 1. Schematic representation of the thermal CVD (Thermal Chemical Vapor Deposition) system with indication of the main components: 1- Horizontal thermal reactor; 2 - Programmable control unit of the thermal reactor; 3 - Cylindrical quartz tube; 4 - Valve for vacuum pumping and substrate loading; 5 - Gas precursor delivery system; 6 - Vacuum system; 7 - Chiller (cooling system).

Inside the reactor, a cylindrical quartz tube (3) surrounded by a heating element is installed, providing uniform heating of the substrates to temperatures between 300 ^{0}C and 1200 °C, which are required for homogeneous deposition. The quartz tube is resistant to high temperatures and chemical exposure, preventing contamination of the substrates. One end of the tube is connected to a valve for vacuum pumping and substrate loading (4), which ensures system sealing and allows substrates to be loaded or unloaded while maintaining either vacuum or atmospheric pressure, depending on the operating mode. To initiate the reaction of gaseous precursors, a gas precursor delivery system (5) is employed; it regulates the introduction of gases such as argon (Ar), hydrogen (H_2), and methane (CH_4) from cylinders through pressure regulators and mass flow controllers, ensuring precise control of the gas mixture. On the opposite side of the reactor, a vacuum system (6) equipped with a pump maintains low pressure (0.1–10 Torr for CVD), removing by-products and residual air. The entire gas delivery and reactor control system is cooled using a chiller (cooling system) (7), which prevents overheating of components and extends the service life of the equipment. Characterization of the microstructure and surface features of the obtained samples was performed using a Nikon L150 optical microscope equipped with a Nikon Digital Sight DS-U digital camera; a field-emission

scanning electron microscope (FESEM, JSM-6500F, Japan); and Raman spectroscopy using a confocal Raman microscope System 1000 (Raman Microscope, Renishaw plc, UK). Raman spectra were acquired at room temperature using excitation wavelengths of 514 nm and 785 nm from iodine lasers. The spatial resolution was better than <1 nm, and the laser spot size ranged between 0 and 250 nm. Spectra were recorded from the graphene surface in the range of 100–3000 cm^{-1}, and each analyzed area was simultaneously imaged with an optical microscope.

RESULTS

The morphology of initial copper foil before CVD treatment measured by scanning electron microscope and optical microscope images illustrated in Figure 2 (a) and (b). According to the images of SEM, the surface of the cleaned copper foil is uniform. In spite of metallic surface of the sample polished and cleaned by ultrasound, but at the same time had small residual strips of rolled metal. There are small longitudinal strips are observed on surface (before polishing) caused by rotation, elongation and pressure of the rolling shafts (see image b,d). In general, the morphology of the sample is identical over the entire surface Figure 2 (a,c). Local elemental analysis of the surface of the samples shown in right upper corner of Figure 2 (a). It was observed that following ratio of the starting components consist from copper having an atomic weight of up to 97 percent, while the oxygen content reaches up to 3 atomic percent before thermal treatment in CVD chamber Figure 2 (a).

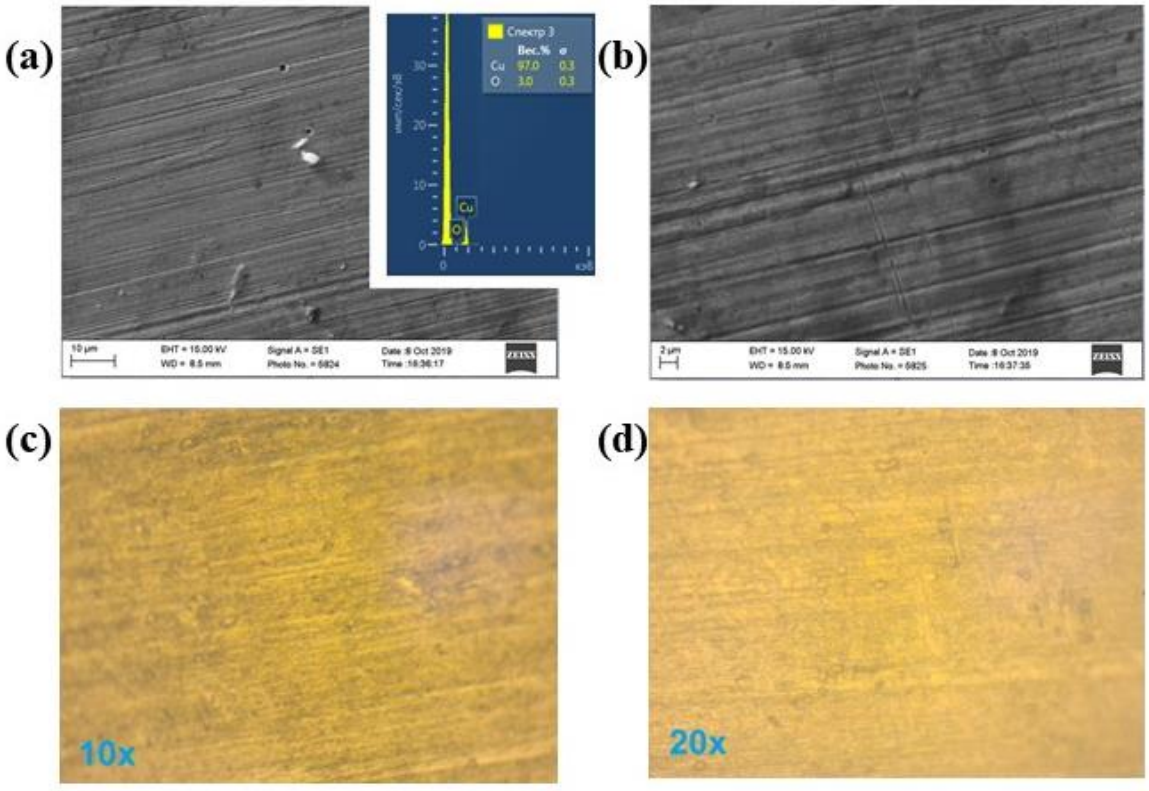

Figure 2. SEM images of cleaned initial copper surfaces (a,b) and optical image of cleaned copper foil before electrochemical anodizing (local elemental composition in the right upper corner of (a)).

Figure 3 presents the XRD patterns of initial copper foil. The XRD patterns were analyzed using the HighScore software and compared with the PDF-2 database (2013 edition). The diffraction peaks are sharp and narrow, indicating a high degree of crystallinity metallic copper phases of initial copper foil. This copper foil primarily consists of metallic copper,

corresponding to the (PDF-2 database pattern 03-065-9743), along with a minor presence of copper oxide (PDF-2 database 01-077-7716).

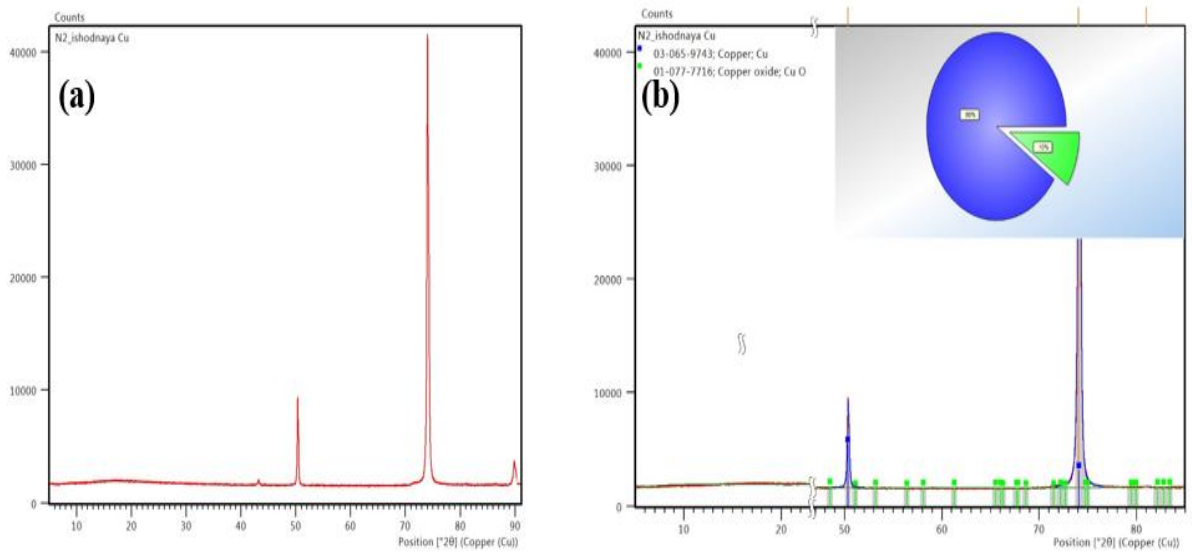

Figure 3. XRD patterns of initial copper foil: (a)- distribution peaks among 5-90 degree; (b)- patterns were analyzed using the HighScore software and compared with the PDF-2 database.

Graphene synthesis was carried out by chemical vapor deposition (CVD) on a copper substrate. For this purpose, copper foil (99.99%) with a thickness of 1 mm and cut into 4 × 6 cm pieces was used as the substrate. The choice of copper is attributed to the fact that, under specific orientations and technological conditions of vapor-phase deposition, graphene is formed with a structure that depends on the crystalline orientation of copper [43–45]. Prior to loading into the reactor, the substrate underwent sequential cleaning in acetone, isopropyl alcohol, and distilled water. This was followed by purging with an argon gas flow and drying at 80 ^{0}C for 60 minutes. After the cleaning procedure, the copper substrate was placed into the horizontal reactor of the CVD system. The reactor consists of a heating furnace with thermal insulation composite material and a metallic housing, inside which a horizontally positioned quartz cylindrical tube with a length of up to 150 cm and a diameter of approximately 20 cm is installed. On one side of the horizontal reactor, feeds for the precursor and cooling gas were introduced, and a thermocouple rod was mounted such that its tip was located directly above the substrate. On the opposite side, a vacuum pump was connected, and a loading valve for introducing samples was installed.

During operation of the CVD system, three thermal zones are formed inside the reactor, with the highest temperature located in the central region. Temperature control of the heating zone was maintained using a temperature regulator operating in the range of 10–1200 ^{0}C with an accuracy of ±0.5 ^{0}C. Graphene growth in the CVD setup was performed according to the scheme shown in Figure 4. The copper substrate was placed horizontally in the center of the reaction chamber, followed by preliminary pumping using a fore-vacuum pump. After reaching a pressure of 1–4 Torr and achieving the required heating temperature, graphene synthesis was initiated, consisting of five stages:

1. Heating the reactor to 300 ^{0}C under preliminary vacuum.
2. Introduction of hydrogen gas (H_2, 20–30 sccm) followed by thermal heating to 500 ^{0}C (as shown in Figure 4) to remove the oxide layer from the surface of the copper substrate. Hydrogen molecules in the reaction medium facilitate the removal of copper oxidation by-products and contribute to the stabilization of graphene growth. The thermal treatment was carried out for one hour.

3. Further increase of temperature to 990 ^{0}C. Upon reaching the optimal temperature, the system parameters (temperature and pressure) were stabilized, followed by annealing of the copper substrate. During annealing at 990 ^{0}C under a hydrogen flow of 20–30 sccm and a pressure of up to 5 mTorr, improvement in the crystalline quality and enlargement of the copper grain size occur.

4.

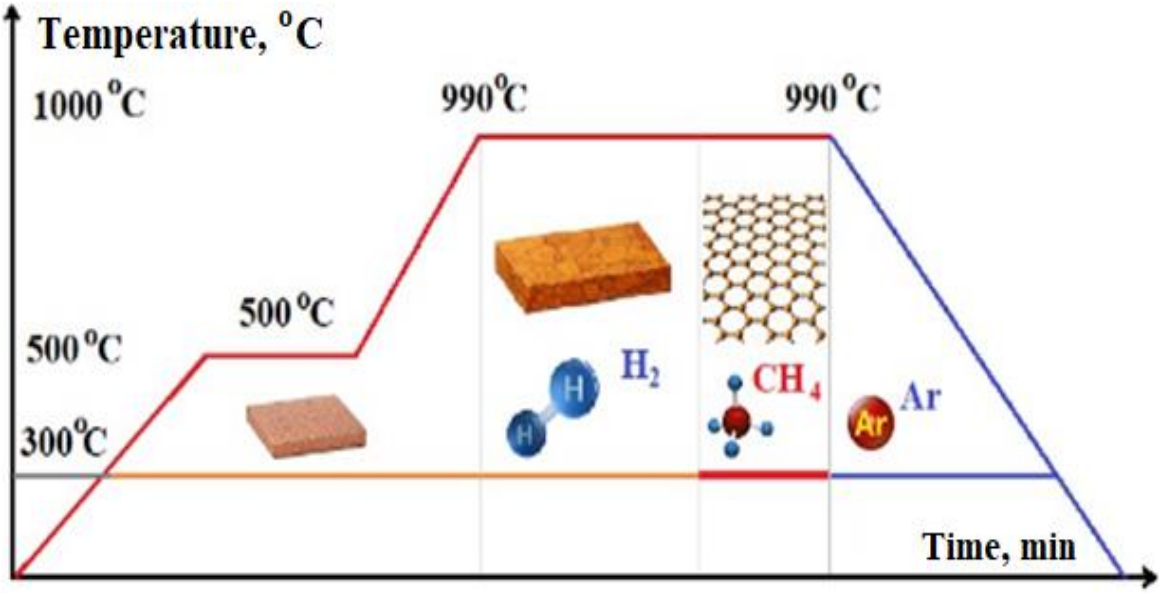

5.

6.

Figure 4. Schematic representation of the graphene growth process on a copper substrate.

7. After thermal annealing in a hydrogen flow, methane gas (CH_4, 20–40 sccm) was introduced into the reactor as a precursor for 30 minutes at a pressure of 1–5 mTorr. At this stage, graphene films were formed on the grains of the copper substrate. Literature sources report the use of various precursor solutions for the synthesis of graphene films [46].

8. Upon completion of graphene domain growth, the methane flow was switched off and an argon flow was introduced to optimize the cooling rate. In this case, the temperature decreased exponentially to 200 ^{0}C within 25–30 minutes. This is due to the fact that slow cooling alters the structure of the graphene film and degrades its crystallinity [44-45].

As the graphene layer grows, it acts as a barrier preventing further carbon deposition, leading to the formation of predominantly monolayer graphene. This property makes copper a unique substrate compared to other metals such as nickel or cobalt. The mechanism of graphene growth on a copper substrate can be explained by considering the catalytic properties of copper and the kinetics of the process. Figure 5 illustrates four key stages of the mechanism of graphene domain growth on a copper substrate, each of which is described below. In the initial stage, the copper substrate is typically covered with a thin oxide layer (Cu_2O or CuO), formed through interaction with the ambient environment. This oxide layer can hinder graphene adhesion and deteriorate the crystalline quality. Preliminary thermal treatment is performed at 200–300 ^{0}C in a hydrogen (H_2) flow, which effectively reduces the oxide to metallic copper. In Figure 5 (transition 1–2), this stage is shown as a substrate with a bluish oxide layer that is removed, exposing a clean copper surface with a roughened texture.

Subsequent treatment at 500 ^{0}C in hydrogen further improves the crystalline structure and increases the grain size of the copper substrate. At this stage, shown in Figure 5 (transition 1-2), thermal annealing enhances the crystalline structure of copper by enlarging grain size and reducing defects such as grain boundaries and dislocations. Increasing the copper grain size

promotes the formation of larger and more uniform graphene domains in the subsequent stages of growth.

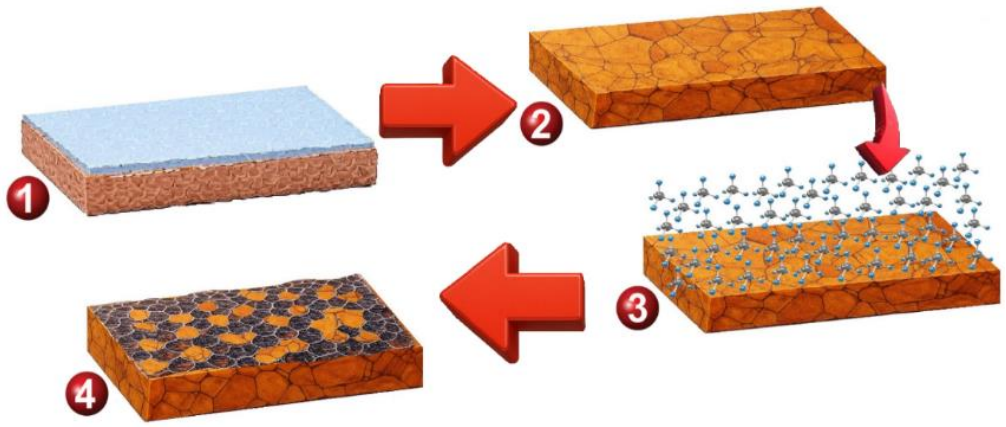

Figure 5. Mechanism of graphene domain growth on a copper substrate 1 - Preliminary thermal treatment; 2 - Annealing at 990 °C in a hydrogen flow; 3 - Catalytic decomposition of methane followed by carbon deposition onto the heated copper surface; 4 - Formation of crystalline graphene domains.

After the oxide layer is removed and the crystal grains are enlarged, the substrate undergoes annealing at high temperature (approximately 990 ^{0}C) in a hydrogen (H_2) atmosphere. In Figure 5 (transition 2-3), the substrate is shown with a more pronounced texture, reflecting the reorganization of the copper crystal lattice under the influence of high temperature and hydrogen. Hydrogen plays a dual role. First, it reduces copper oxide and prevents re-oxidation during annealing. Second, it acts as an etchant, removing excess amorphous carbon and promoting the growth of crystalline graphene domains. The optimal H_2/CH_4 ratio (typically 1:5–1:15) is critical for controlling the film thickness. The next stage involves the catalytic decomposition of methane followed by carbon deposition onto the heated copper surface, as illustrated in Figure 5 (transition 3–4). At this stage, methane (CH_4) is introduced into the reactor as the carbon source at 990 ^{0}C. Copper acts as a catalyst, facilitating methane decomposition $CH_4(g) \rightarrow C(\text{graphene}) + 2H_2(g)$ on its surface. The released carbon atoms diffuse along the surface and begin to aggregate as graphene islands. Hydrogen present in the gas mixture prevents excessive deposition of amorphous carbon and promotes the formation of crystalline structures. In this case, carbon atoms are liberated, diffuse across the surface, and recrystallize into a graphene structure. Thus, in Figure 5, the copper surface is depicted as being covered with methane molecules that decompose and deposit carbon atoms through catalytic dissociation of methane at the copper interface. In the final stage, carbon atoms deposited onto the copper surface self-assemble into hexagonal as well as rectangular graphene domains. The process is self-limiting: the low solubility of carbon in copper restricts its diffusion into the bulk, resulting in the formation of predominantly domain-structured graphene. The size and shape of the domains depend on temperature, gas ratios, and exposure time. In Figure 5 (transition 3-4), the copper substrate is shown with well-defined hexagonal patterns representing graphene domains.

Figure 6 presents the results of microstructural analysis of the copper substrate surface obtained by optical microscopy and scanning electron microscopy (SEM) after processing in the chemical vapor deposition reactor. The optical microscopy image (scale 100 μm) and the SEM image (scale 10 μm) in Figure 6(a) show individual darkened discrete regions of varying orientation on the copper substrate, corresponding to multilayer graphene domains. Further magnification in the SEM images at scales of 10 μm and 1 μm (see inset in the upper right corner of Figure 6(a), (b)) identifies continuous domains of multilayer graphene with

heterogeneous growth directions. The enlarged inset in Figure 7(b) reveals that most domains exhibit quasi-rectangular morphology. The dimensions of multilayer graphene domains vary within the range of 10 -100 μm. It is evident that the degree of orientation and clustering of graphene domains depends on the crystallographic orientation of the copper substrate.

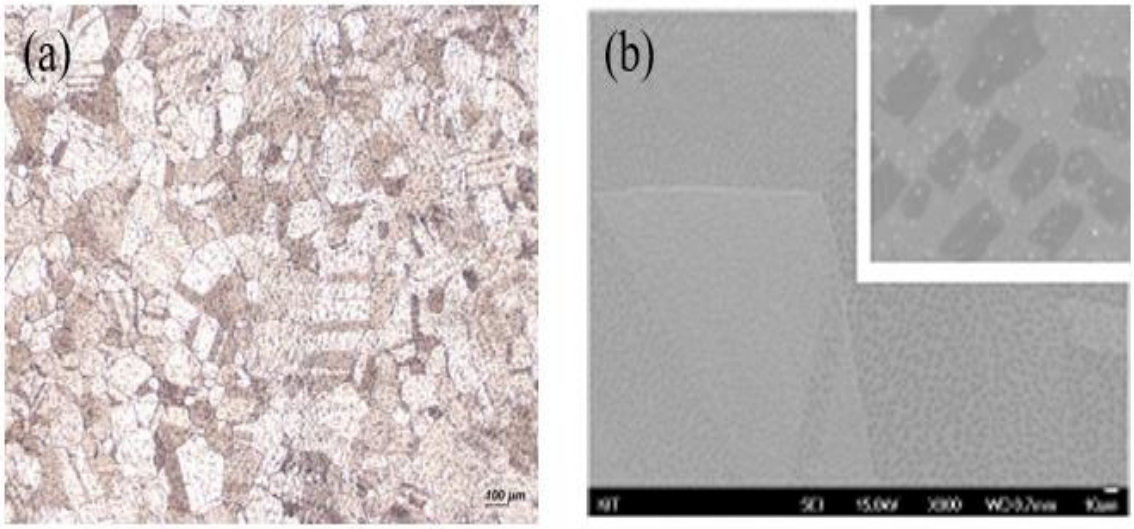

Figure 6. Surface image of the copper substrate obtained using optical microscopy (a) and scanning electron microscopy (b) after processing in the chemical vapor deposition reactor under precursor gas flow.

Figure 7 shows the elemental composition spectrum and the image of the selected local region. Analysis of the composition in the local area corresponding to spectrum 4 on the surface of the copper plate revealed an elemental composition in which carbon accounts for more than 16 at.% and copper for 84 at.%.

Element	Weight%	Atomic%
C K	3.49	16.06
Cu L	96.51	83.94
Totals	100.00	

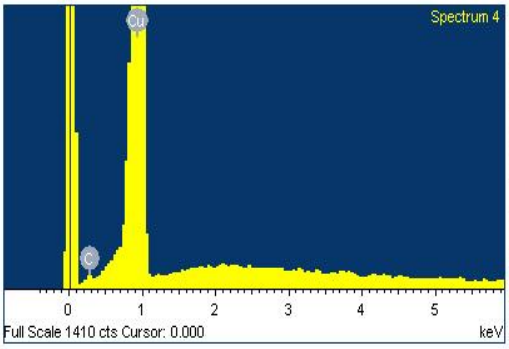

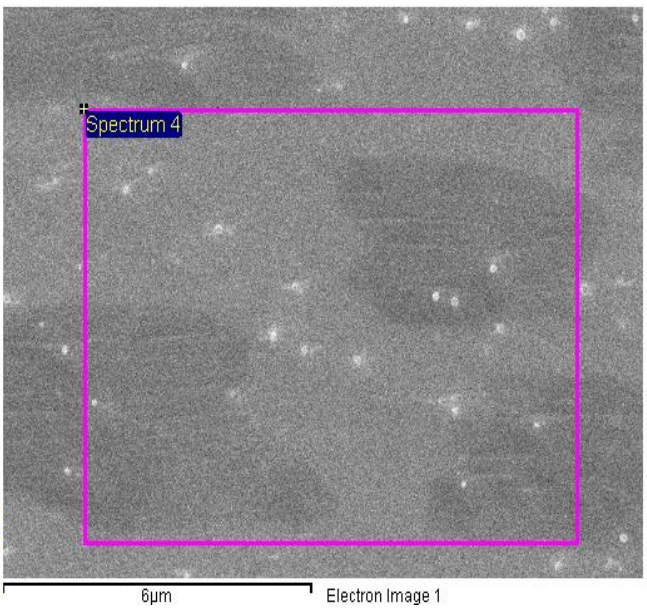

Figure 7. Elemental composition at a local region on the surface of the copper substrate after graphene growth in the chemical vapor deposition reactor under precursor gas flow.

Raman spectroscopy (RS) is a powerful tool for characterizing the structural properties of graphene, including defect density and the number of layers, as reported in previous studies of carbon-based materials. The Raman spectra of the copper substrate on which graphene domains were grown by chemical vapor deposition are presented in Figure 8. For graphene, three characteristic bands are typically observed in Raman spectra: the G band, the D band, and the 2D band [2, 4, 43-45].

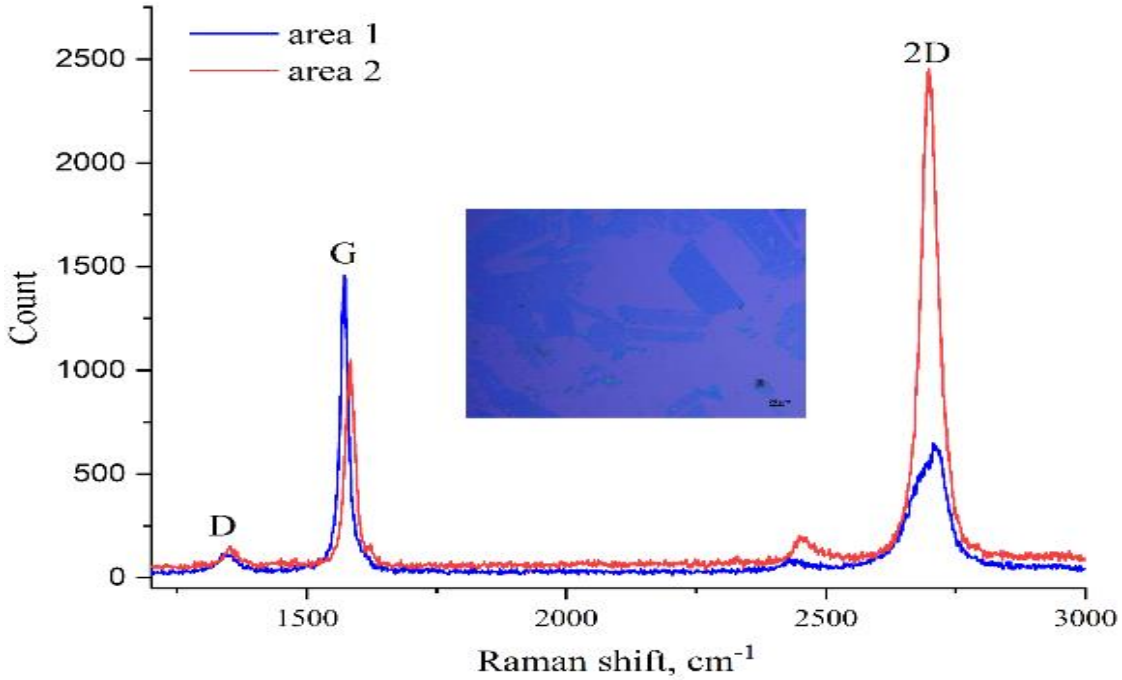

Figure 8. Raman spectroscopy of graphene at different regions of the copper substrate surface.

The inset image within the graph shows the appearance of the graphene sample surface obtained using optical microscopy, which provides contextual visualization of the analyzed regions. In addition, the presence of a weak D peak (1350 cm^{-1}) in the Raman spectra, as well as its broadening, indicates the presence of defects within the graphene domains, arising from structural disorder formed during high-temperature thermal treatment in a methane atmosphere in the chemical vapor deposition reactor. Furthermore, a pronounced G band (1582 cm^{-1}) is observed, which is attributed to a high degree of crystallization in localized areas, as well as to the in-plane vibrational mode of sp^2-bonded carbon atoms, which is a characteristic feature of carbon-based materials. The 2D band (2700 cm^{-1}) appears broader and asymmetric, indicating the formation of multilayer graphene in the investigated material. The intensity ratio of the D and G bands, I_D/I_G, is approximately equal to one, which further confirms the presence of a heterogeneous structure with non-uniformly oriented graphene domains [45]. This is due to the fact that the 2D band near 2700 cm^{-1} represents the second overtone of the D band and is extremely sensitive to the number of graphene layers, making it a key indicator of layer thickness.

Transfer graphene domains to silicon substrate. In order to transfer graphene onto a silicon substrate, a technological process was used involving the deposition of polymethyl methacrylate (PMMA), etching of the copper substrate, and removal of the organic coating, followed by transfer onto the silicon substrate. The stages of this process are schematically shown in Figure 9 and will be discussed in more detail below. The study of the growth of non-uniform domains on the surface of the copper substrate is an important process in the formation

of graphene films on copper. At the same time, the transfer onto a solid substrate is of great importance in the fabrication technology. In this work, we consider the process of transferring graphene domains using organic binding materials. Therefore, for further investigation of the grown graphene, a transfer process onto a separate substrate must be carried out. In such cases, polymer adhesive films are usually used, which are applied to the substrates on which graphene is grown. After that, the substrate itself is removed, resulting in a polymer film attached to the graphene [44-45]. This structure can be transferred onto the desired substrate for further study. The schematic of this technological process is shown in Figure 9.

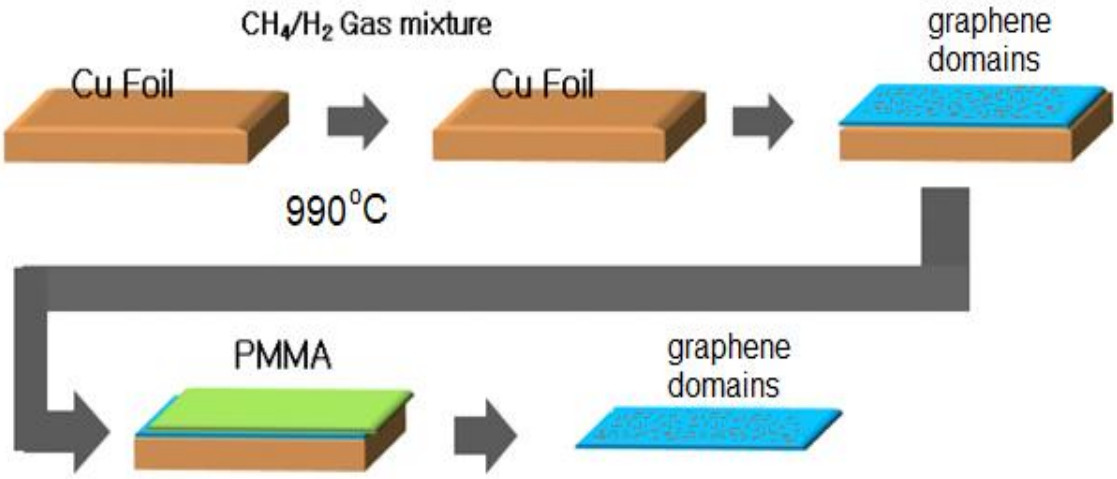

Figure 9. Schematic illustration of the sequence of the graphene domain transfer process onto a solid substrate.

To study the functional features of the synthesized graphene, a transfer process onto an isolated SiO_2/Si substrate was carried out by applying an adhesive agent and etching the substrate. A polymer film made of polymethyl methacrylate (PMMA) was used for the coating, enabling the capture of individual multilayer graphene domains after etching of the copper substrate. The polymer coating was applied by spin-coating at speeds up to 2500 rpm followed by drying in an oven. Once the surface of the sample was uniformly covered with a polymer film about ~0.5 mm thick, the original substrate was etched in a nickel etchant solution. The etching of the copper took 30–60 minutes, and the PMMA film with graphene freely floated on the surface of the etchant. The separated polymer film with graphene was washed in distilled water and transferred onto an SiO_2/Si substrate. Then the SiO_2/Si–graphene–PMMA structure was dried in an oven at 50 ^{0}C for 3 hours. This method allowed complete transfer of the synthesized graphene onto a separate insulating substrate. Afterwards, the PMMA was removed in a solution of dichlorobenzene (Sigma-Aldrich), followed by drying at 150 ^{0}C for 30 minutes in air. Then, the morphology of the obtained graphene film on the isolated SiO_2/Si substrate was examined. Figure 10 shows images of the sample surface obtained by optical and scanning electron microscopy before dissolving the PMMA film in dichlorobenzene, and Figure 10 shows the images after dissolution.

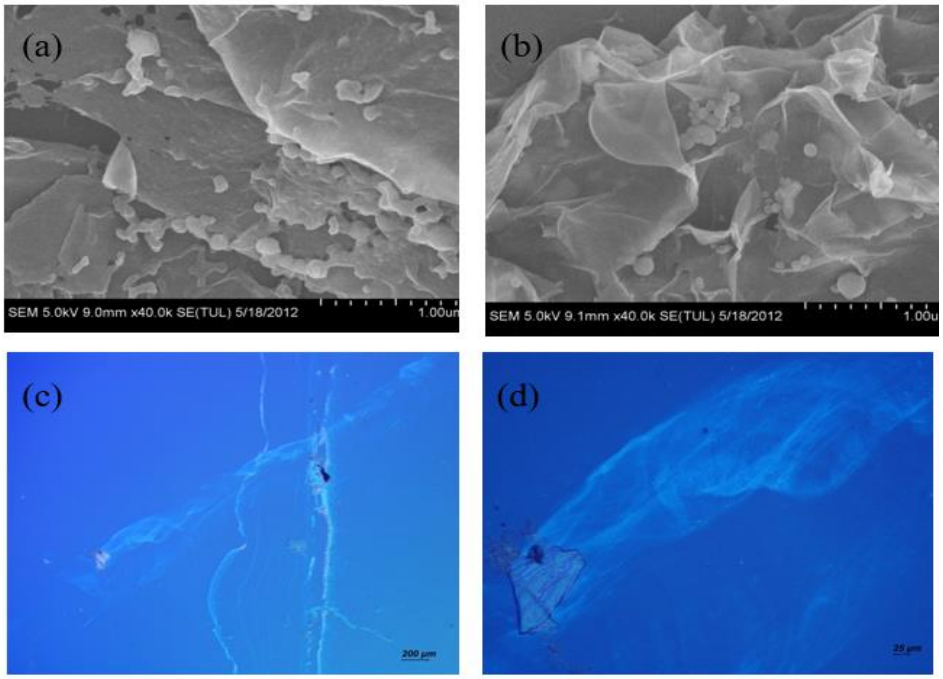

Figure 10. Morphology obtained by optical and scanning electron microscopy of graphene domain films after transfer onto an isolated SiO_2/Si substrate before PMMA dissolution (a) and (c), and after dissolution (b) and (d) in dichlorobenzene.

As seen in Figures 11(a) and 11(b), despite the spin-coating process used for applying the polymer coating, heterogeneous wrinkles and irregularities of the films are observed on the surface, as well as some blistering after drying. This indicates that the thin polymer coating

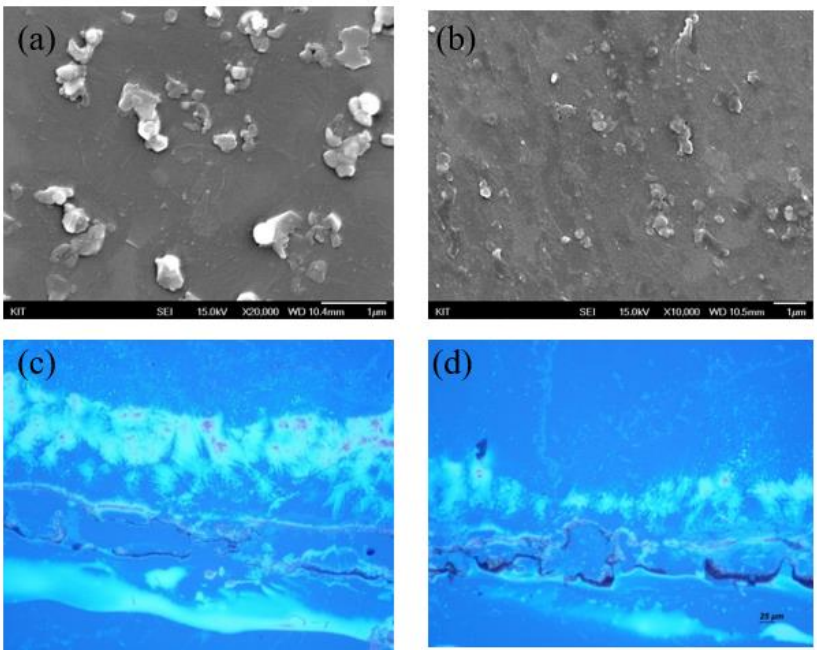

Figure 11. Morphology obtained by optical and scanning electron microscopy of graphene domain films after transfer onto an isolated SiO_2/Si substrate before PMMA dissolution (a) and (c), and after dissolution (b) and (d) in dichlorobenzene.

significantly affects the cleanliness of the graphene domain transfer: the wrinkles and accumulations of organic film formed after application and drying contaminate the surface and have a detrimental effect on the original properties of the films.

As a result, after removing the PMMA film with dichlorobenzene, islands and residues of undissolved PMMA organic film were observed at locations where wrinkles and irregularities had formed (see Figure 11 (a -d)). This, in turn, contaminates the surface of the material under study and leads to deterioration of its functional characteristics, which is critical in nano- and microelectronics. Therefore, it is necessary to explore methods for direct graphene transfer without using any polymer coatings.

CONCLUSIONS

In the present work, a synthesis technology for discrete multilayer graphene domains on a copper substrate using chemical vapor deposition (CVD) has been developed. The optimal process parameters were experimentally determined, including temperature regimes (preheating to 300 °C, annealing at 500 ^{0}C and 990 ^{0}C, and growth at 990 ^{0}C), gas flow rates (H_2 at 20–30 sccm for oxide removal and annealing, CH_4 at 20–40 sccm as a precursor), pressure (1–5 mTorr), and cooling rate using argon (down to 200 ^{0}C within 25–30 minutes). Surface morphology studies conducted by optical and scanning electron microscopy revealed the formation of rectangular graphene domains sized 10–100 μm with heterogeneous orientations dependent on the crystalline structure of the copper substrate. Raman spectroscopy confirmed the multilayer nature of the graphene (broad asymmetric 2D band near 2700 cm^{-1}, $I_D/I_G \approx 1$), the presence of defects (weak D band around 1350 cm^{-1}), and a high degree of crystallinity (G band near 1582 cm^{-1}). Elemental analysis showed a carbon content of approximately 16 at.% on the surface. The obtained results demonstrate the efficiency of the CVD method for large-area graphene synthesis on copper substrates, highlighting its potential applications in electronics, sensors, and energy-related technologies. To study the functional features of the synthesized sample, graphene was transferred onto an isolated SiO_2/Si substrate. A controlled CVD process for synthesizing discrete multilayer graphene domains on copper substrates has been developed and optimized. Surface characterization confirmed the formation of rectangular graphene domains with heterogeneous orientation dictated by the copper crystallography. Raman spectroscopy verified the multilayer nature and defectiveness of the domains. For this purpose, a polymer film of polymethyl methacrylate was applied to the surface of the copper substrate with graphene domains by the spin-coating method, followed by etching of the copper substrate in an etchant solution. Then, the PMMA–graphene structure was transferred onto the SiO_2/Si substrate, after which the polymer film was dissolved in a dichlorobenzene solution. The results of optical and scanning microscopy showed that the surface of the graphene–SiO_2/Si structure is contaminated with discontinuous wrinkles and islands of organic matter, formed as residues of the undissolved polymer film. In this regard, when synthesizing graphene films by chemical vapor deposition, the use of polymer coatings should be avoided, and the process of transferring graphene onto an isolated substrate should be carried out directlyFuture studies may focus on defect minimization and optimization of graphene transfer onto alternative substrates. PMMA-assisted transfer to SiO_2/Si introduced structural distortions and organic contamination, underscoring the limitations of polymer-based transfer methods. Future work will focus on developing direct, residue-free transfer strategies and improving the uniformity of graphene growth for applications in electronic, sensing, and energy devices.

The research results were obtained within the framework of the dissertation work of O.M. Tursunkulov. This work was supported by the Korea International Cooperation Agency (KOICA) within the framework of a joint project with the Korea Research Institute of Chemical Technology (KRICT) and the Center for Advanced Technologies (CAT).

REFERENCES

1. Geim, A.K. and Novoselov, K.S., 2007. The rise of graphene. *Nature Materials*, 6, pp.183–191.
2. Geim, A.K., 2009. Graphene: status and prospects. *Science*, 324, pp.1530–1534.
3. Singh, V., Daehajoung, L., Zhai, L., Das, S., Khondaker, S.I. and Seal, S., 2011. Graphene based materials: past, present and future. *Progress in Materials Science*, 56, pp.1178–1271.
4. Huang, X., Yin, Z., Wu, S., Qi, X., et al., 2011. Graphene-based materials: synthesis, characterization, properties, and applications. *Small*, 7(14), pp.1876–1902.
5. Mattevi, C., Kim, H. and Chhowalla, M., 2011. A review of chemical vapour deposition of graphene on copper. *Journal of Materials Chemistry*, 21, pp.3324–3334.
6. Brownson, D.A.C., Kampouris, D.K. and Banks, C.E., 2011. An overview of graphene in energy production and storage applications. *Journal of Power Sources*, 196, pp.4873–4885.
7. Kashyap, A. et al., 2025. Recent progress on graphene-based derivatives for enhanced [full title not specified]. *[Journal not specified]*, 202401794, pp.1–49.
8. Neto, A.C., Guinea, F., Peres, N.M.R., Novoselov, K.S. and Geim, A.K., 2009. The electronic properties of graphene. *Reviews of Modern Physics*, 81, pp.109–116.
9. Urade, A.R., Lahiri, I. and Suresh, K.S., 2023. Graphene properties, synthesis and applications: a review. *JOM*, 75(3), pp.614–630.
10. Novoselov, K.S., Geim, A.K., Morozov, S.V., Jiang, D., Zhang, Y., Dubonos, S.V., Grigorieva, I.V. and Firsov, A.A., 2004. Electric field effect in atomically thin carbon films. *Science*, 306, pp.666–669.
11. Jain, P. et al., 2024. Recent advances in graphene-enabled materials for photovoltaic applications: a comprehensive review. *ACS Omega*, 9(11), pp.12403–12425.
12. Muchuweni, E. et al., 2025. Towards high-performance dye-sensitized solar cells by utilizing reduced graphene oxide-based composites as potential alternatives to conventional electrodes: a review. *Next Materials*, 6(December 2024), p.100477.
13. De Arco, L.G., Zhang, Y., Schlenker, C.W., Ryu, K., Thompson, M.E. and Zhou, C., 2010. Continuous, highly flexible, and transparent graphene films by chemical vapor deposition for organic photovoltaics. *ACS Nano*, 4(5), pp.2865–2873.
14. Pasadas, F. et al., 2023. Exploiting ambipolarity in graphene field-effect transistors for novel designs on high-frequency analog electronics. *[Journal not specified]*, 2303595, pp.1–15.
15. Kiranakumar, H.V., Thejas, R., Naveen, C.S., Khan, M.I. et al., 2024. A review on electrical and gas-sensing properties of reduced graphene oxide-metal oxide nanocomposites. *Biomass Conversion and Biorefinery*, 14(12), pp.12625–12635.
16. Park, J., Lee, W.H., Huh, S., Sim, S.H., Kim, S.H., Kim, S.B., Cho, K., Hong, B.H. and Kim, K.S., 2011. Work-function engineering of graphene electrodes by self-assembled monolayers for high-performance organic field-effect transistors. *Journal of Physical Chemistry Letters*, 2, pp.841–845.
17. Lee, W.H., Park, J., Kim, Y., Kim, K.S., Hong, B.H. and Cho, K., 2010. Control of graphene field-effect transistors by interfacial hydrophobic self-assembled monolayers. *Advanced Materials*, 23, pp.3460–3464.
18. Song, I., Kim, Y., Kim, K.S., Ozyilmaz, B., Ahn, J. and Hong, B.H., 2010. Roll-to-roll production of 30-inch graphene films for transparent electrodes. *Nature Nanotechnology*, 5, pp.574–578.
19. Jo, G., Choe, M., Cho, C.Y., Kim, J.H., Park, W., Lee, S., Lee, T. et al., 2010. Large-scale patterned multi-layer graphene films as transparent conducting electrodes for GaN light-emitting diodes. *Nanotechnology*, 21, p.175201.
20. Recum, P. and Hirsch, T., 2024. Graphene-based chemiresistive gas sensors. *Nanoscale Advances*, 6(1), pp.11–31.

21. Thejas, R. et al., 2024. A review on electrical and gas-sensing properties of reduced graphene oxide-metal oxide nanocomposites. *Biomass Conversion and Biorefinery*, 14(12), pp.12625–12635.
22. Madhav, G. and Jayatissa, A.H., 2011. Gas sensing properties of graphene synthesized by chemical vapor deposition. *Materials Science and Engineering C*, 31, pp.1405–1411.
23. Zhang, H., Fan, L., Dong, H., Zhang, P., Nie, K., Zhong, J., Li, Y., Guo, J. and Sun, X., 2016. Spectroscopic investigation of plasma-fluorinated monolayer graphene and application for gas sensing. *ACS Applied Materials & Interfaces*, 8(13), pp.8652–8661.
24. Basu, S. and Bhattacharyya, P., 2012. Recent developments on graphene and graphene oxide based solid state gas sensors. *Sensors and Actuators B: Chemical*, 173, pp.1–21.
25. Avouris, P., 2010. Graphene: electronic and photonic properties and devices. *Nano Letters*, 10, pp.4285–4294.
26. Jung, I., Pelton, M., Piner, R. et al., 2007. Simple approach for high-contrast optical imaging and characterization of graphene-based sheets. *Nano Letters*, 7, pp.3569–3575.
27. Zheng, Y., Ni, G.X., Bae, S., Cong, C.X., Kahya, O., Hong, B.H. and Ozyilmaz, B., 2011. Wafer-scale graphene/ferroelectric hybrid devices for low-voltage electronics. *EPL (Europhysics Letters)*, 93, p.17002.
28. Sevincli, H., Topsakal, M., Durgun, E. and Ciraci, S., 2008. Electronic and magnetic properties of 3d transition-metal atom adsorbed graphene and graphene nanoribbons. *Physical Review B*, 77, p.195434.
29. Sadiq, I., Ali, S.A. and Ahmad, T., 2023. Graphene-based derivatives heterostructured catalytic systems for sustainable hydrogen energy via overall water splitting. *Catalysts*, 13(1), p.109.
30. Bongu, C.S. et al., 2024. Graphene-based 2D materials for rechargeable batteries and hydrogen production and storage: a critical review. *Sustainable Energy & Fuels*, 8(18), pp.4039–4070.
31. Arya, A.K. et al., 2024. Graphene-coated Ni–Cu alloys for durable degradation resistance of bi-polar plates for proton exchange membrane fuel cells: remarkable role of alloy composition. *Advanced Energy Materials*, 14, p.2305320.
32. Wu, W., Liu, Z., Jauregui, L.A., Yu, Q., Pillai, R., Cao, H., Bao, J., Chen, Y.P. and Pei, S.S., 2010. Wafer-scale synthesis of graphene by chemical vapor deposition and its application in hydrogen sensing. *Sensors and Actuators B: Chemical*, 150(1), pp.296–300.
33. Ilnicka, A. and Lukaszewicz, J.P., 2020. Graphene-based hydrogen gas sensors: a review. *Processes*, 8, p.633.
34. Lonkar, S.P. and Abdala, A.A., 2014. Applications of graphene in catalysis. *Journal of Thermodynamics & Catalysis*, 5(2), p.1000132.
35. Yam, K.M., Guo, N., Jiang, Z., Li, S. and Zhang, C., 2020. Graphene-based heterogeneous catalysis: role of graphene. *Catalysts*, 10, p.53.
36. Jin, M., Jeong, H.K., Kim, T.H., So, K.P., Cui, Y., Yu, W.J., Ra, E. and Lee, Y.H., 2010. Synthesis and systematic characterization of functionalized graphene sheets generated by thermal exfoliation at low temperature. *Journal of Physics D: Applied Physics*, 43, p.275402.
37. Khan, U., O'Neill, A., Lotya, M., De, S. and Coleman, J.N., 2010. High-concentration solvent exfoliation of graphene. *Small*, 6(7), pp.864–871.
38. Peng, X. and Ahuja, R., 2008. Symmetry breaking induced bandgap in epitaxial graphene layers on SiC. *Nano Letters*, 8, pp.4464–4468.
39. Nomani, M.W.K., Shishir, R., Qazi, M., Diwan, D., Shields, V.B., Spencer, M.G., Tompa, G.S., Sbrockey, N.M. and Koley, G., 2010. Highly sensitive and selective detection of NO_2 using epitaxial graphene on 6H-SiC. *Sensors and Actuators B: Chemical*, 150, pp.301–307.

40. Stankovich, S., Dikin, D.A., Piner, R.D., Kohlhaas, K.A., Kleinhammes, A., Jia, Y., Wu, Y., Nguyen, S.T. and Ruoff, R.S., 2007. Synthesis of graphene-based nanosheets via chemical reduction of exfoliated graphite oxide. *Carbon*, 45, pp.1558–1565.
41. Moradizadeh, L., Yazdanpanah, P. and Karimi, G., 2023. Investigating the role of graphite and reduced graphene oxide in the fabrication of microporous layers for proton exchange membrane fuel cells. *Journal of Materials Science*, 58(31), pp.12706–12723.
42. Kim, E., Lee, W.G. and Jung, J., 2011. Agglomeration effects of thin metal catalyst on graphene film synthesized by chemical vapor deposition. *Electronic Materials Letters*, 7(3), pp.261–264.
43. Wang, Y. et al., 2011. Electrochemical delamination of CVD-grown graphene film: toward the recyclable use of copper catalyst. *ACS Nano*, 5(12), pp.9927–9933.
44. Ishihara, M., Koga, Y., Kim, J., Tsugawa, K. and Hasegawa, M., 2011. Direct evidence of advantage of Cu (111) for graphene synthesis by using Raman mapping and electron backscatter diffraction. *Materials Letters*, 65, pp.2864–2867.
45. Kim, W., Yoo, K., Seo, E.K., Kim, S.J. and Hwang, C., 2011. Scanning tunneling microscopy study on a graphene layer grown on a single-crystal Cu (111) surface by using chemical vapor deposition. *Journal of the Korean Physical Society*, 59(1), pp.71–74.
46. Guermoune, A., Chari, T., Popescu, F., Sabri, S.S., Guillemette, J., Skulason, H.S., Szkopek, T. and Siaj, M., 2011. Chemical vapor deposition synthesis of graphene on copper with methanol, ethanol, and propanol precursors. *Carbon*, 49, pp.4204–4210.
47. Miyata, Y., Kamon, K., Ohashi, K., Kitaura, R., Yoshimura, M. and Shinohara, H., 2010. A simple alcohol-chemical vapor deposition synthesis of single-layer graphenes using flash cooling. *Applied Physics Letters*, 96, p.263105.